




## Original article

# Water activity and glass transition effect on the physical properties and bioactive compounds of persimmon peel powder

Sepideh Hosseinijad, Virginia Larrea, Amparo Quiles, Isabel Hernando\*  & Gemma Moraga

Department of Food Science and Technology, Universitat Politècnica de València, Camino de Vera, s/n 46021, Valencia, Spain

(Received 13 October 2023; Accepted in revised form 31 January 2024)

**Summary** Persimmon peel is an agro-industrial by-product that could be valorised as a potential powdered functional ingredient. However, powdered products exhibit quality and stability problems associated with the water activity and the glass transition. In this work, hot-air drying was used to produce a persimmon peel powder, which was conditioned at 20 °C at different relative humidity (11.3%–75.5%). The changes in physical properties (water sorption, glass transition, mechanical properties), structure (light microscopy) and bioactive compounds (soluble tannin content, total carotenoid content) were evaluated. By combining the GAB sorption model and the Gordon and Taylor equation, the critical values of water activity ( $a_w = 0.211$ ) and water content (0.029 g water g<sup>-1</sup> product), related to the glass transition, were obtained. These values were critical for the production of a free-flowing powder rich in bioactive compounds and high antioxidant capacity.

**Keywords** Antioxidant capacity, by-product, caking, glassy–rubbery state, water sorption.

## Introduction

Persimmon (*Diospyros kaki* Thunb.) is consumed in many countries around the world. China is the main producer, followed by Spain, the Republic of Korea and Japan (FAO, 2021). Persimmon production is concentrated in a short period of the year; therefore, persimmon industrialisation is needed to reduce post-harvest losses. The current challenge of the persimmon industry is to increase crop profitability, creating new opportunities to build a more sustainable system that contributes to the circular economy (Hosseinijad *et al.*, 2022a).

The most important persimmon processed product is traditional semi-dried persimmon, which is commonly produced and consumed in Asian countries (Matsumoto *et al.*, 2007; Oh *et al.*, 2018). The procedure followed to obtain most of the semi-dried persimmon and other persimmon-derived products comprises peeling, which results in a high amount of persimmon peel as an agro-industrial by-product, at least 10%, according to Ye *et al.* (2022). Untreated peel is an agricultural waste that poses a serious environmental risk. However, it is necessary to understand the long-term value of peel because it is rich in compounds with nutritional interests (Ohguchi *et al.*, 2010). The main

component of the persimmon peel is dietary fibre, but it also contains vitamins, minerals, polyphenolic compounds (mainly tannins such as proanthocyanidins) and carotenoids (Gorinstein *et al.*, 2001; Smrke *et al.*, 2019). The quantity of bioactive compounds, especially carotenoids and polyphenols, is higher in the peel than in the pulp (Yaqub *et al.*, 2016). These bioactive compounds play an important role in preventing oxidation (Suzuki *et al.*, 2005). Moreover, carotenoids serve as chemo-preventive anticancer (Raskin *et al.*, 2002), anti-inflammatory and immunomodulatory agents (Miller *et al.*, 2004; Yaqub *et al.*, 2016), and polyphenols are receiving a lot of attention because of their ability to reduce cardiovascular diseases (Yaqub *et al.*, 2016).

By processing through simple technology, this by-product could be reintroduced to the production line as a potential functional ingredient with health benefits, improving the nutritional profile of different foods (Del Rio Osorio *et al.*, 2021). Because of its simplicity and affordability, hot-air drying is the most common technique used to obtain food ingredients with an extended shelf life. The primary goal of drying is to remove water from the solids to a point where microbial spoilage and chemical degradative reactions are greatly reduced (Krokida & Marinos-Kouris, 2003). Characterising the water sorption isotherm is critical for determining the stability and acceptability of food

\*Correspondent: E-mail: [mihernan@tal.upv.es](mailto:mihernan@tal.upv.es)

goods, determining moisture changes that may occur during storage and selecting packing materials (Bah-loul *et al.*, 2008). Several mathematical models, both theoretical and empirical, have been proposed to this purpose. Among them, the Brunauer–Emmett–Teller (BET) and the Guggenheim–Anderson–de Boer (GAB) models, are the most widely used in food systems. However, it is recommended to test the ability of several sorption models, since the best equation to describe the water sorption behaviour depends on the food matrix (Collazos-Escobar *et al.*, 2022). Furthermore, to predict the physical and chemical changes in the dehydrated powdered products, it is important to analyse the state of the amorphous phase, which is commonly formed during the rapid water removal associated with the drying process. In terms of product quality and stability, keeping the product below its glass transition temperature ( $T_g$ ) is recommended, because the change from a glassy to a rubbery state has been linked to changes in food physical properties, particularly diffusional and mechanical properties. In the rubbery state, solute crystallisation and/or collapse-related phenomena, such as powder stickiness and caking, may occur (Roos, 1995). Molecular mobility drastically increases, so reactants can diffuse more easily and participate in deterioration reactions. Therefore, the glassy state avoids quality changes in food powders. The increase in the water content and water activity ( $a_w$ ) leads to a decrease in  $T_g$ , due to the plasticisation effect of the water, well characterised by the Gordon and Taylor model. Thus, the relationship between those variables, represented in a modified state diagram, is useful to optimise food formulation and establish processing and storage conditions.

The aim of this work was to study the effect of water content,  $a_w$ , and glass transition on the physical properties and bioactive compounds of persimmon peel powder produced through hot-air drying. The water sorption isotherm and the state diagram of the amorphous phase were used to obtain the critical value of the water content and  $a_w$  needed to guarantee the glassy state of the powdered product.

## Materials and methods

### Sample preparation

Persimmon (*Diospyros kaki* Thunb. cv. Rojo Brillante) fruits were washed and peeled. The peels were hot-air-dried using a tray dryer (Model FED 260 Avantgarde Line, Binder GmbH, Tuttlingen, Germany) with air circulation at 45 °C, 2 m s<sup>-1</sup>, for 22 h until constant weight. After drying, a grinder mill (Moulinex, Barcelona, Spain) was used to obtain a powdered product, which was conditioned to different  $a_w$  levels following the methodology described by González *et al.* (2020).

The equilibrium moisture content was determined considering the initial water content and the weight difference until the equilibrium. The initial water content was obtained by drying the sample in a vacuum oven at 60 °C (Vaciotem, JP Selecta SA, Abrera, Spain). The equilibrated samples were analysed after 5 months of storage. All analyses were performed in triplicate.

### Sorption isotherms

The BET, GAB, Henderson and Caurie models (eqns 1–4, respectively) were used to fit the relationship between  $a_w$  and the equilibrium water content ( $w_e$ , g water g<sup>-1</sup> dry solids) at 20 °C. Statistical software Solver (Excel 2019) was employed for nonlinear regression analysis, minimising the residual sum of squares.

$$w_e = \frac{w_o C a_w}{(1-a_w)(1+(C-1)a_w)} \quad (1)$$

Where,  $w_o$  is the monolayer moisture content (g water g<sup>-1</sup> dry solids), and  $C$  is the sorption energy constant.

$$w_e = \frac{w_o C K a_w}{(1-K a_w)(1+(C-1) K a_w)} \quad (2)$$

Where,  $w_o$  is the monolayer moisture content (g water g<sup>-1</sup> dry solids), and  $C$  is the sorption energy constant related to monolayer sorption and  $K$  is the sorption energy constant related to multilayer sorption.

$$w_e = \left( \frac{-\log(1-a_w)}{10^f} \right)^{1/n} \quad (3)$$

Where,  $n$  and  $f$  are model constants.

$$w_e = \exp \left[ a_w \cdot \ln(r) - \frac{1}{4.5 \cdot w_s} \right] \quad (4)$$

Where,  $r$  is a model constant, and  $w_s$  is the security moisture content (g water g<sup>-1</sup> dry solids).

### Glass transition temperature

The glass transition temperature was obtained by differential scanning calorimetry following the methodology described by Perez-Pirotto *et al.* (2022). The relationship between  $T_g$  (°C) and  $x_w$  (g water g<sup>-1</sup> product) was fitted to the Gordon and Taylor model (eqn 5). Statistical software Solver (Excel 2019) was employed for nonlinear regression analysis, minimising the residual sum of squares.

$$T_g = \frac{(1-x_w) T_{g(as)} + k x_w T_{g(w)}}{(1-x_w) + k x_w} \quad (5)$$

Where,  $T_{g(as)}$  is the glass transition temperature of the anhydrous solids (°C),  $T_{g(w)}$  is the glass transition

temperature of the amorphous water (−135 °C), and  $k$  is the model constant.

### Mechanical properties

A Universal Texture Analyzer (TA.XT2, Stable Micro Systems, Surrey, UK) was selected to study the mechanical behaviour of the equilibrated samples. The powdered samples were poured to fill a cylindrical container 40 mm in diameter by 10 mm in height. A flat-tipped 4 mm cylindrical probe (P/4) was used to penetrate the samples up to a distance of 4 mm at a 1 mm s<sup>−1</sup> rate. The maximum force (N) and the compression area (N·mm) were measured.

### Colour

A Chroma meter CR-400 (Minolta Co., Ltd., Osaka, Japan), with D65 illuminant and 10<sup>0</sup> observer was used to obtain the CIE  $L^*a^*b^*$  colour coordinates. The colour attributes chroma  $C^*$  and hue angle ( $h^*$ ) were calculated using eqns (6) and (7), respectively.

$$C^* = \left[ (a^{*2} + b^{*2})^{1/2} \right] \tag{6}$$

$$h^* = \tan^{-1} \frac{b^*}{a^*} \tag{7}$$

Total colour difference ( $\Delta E^*$ ) was calculated regarding the lowest  $a_w$  ( $a_w = 0.113$ ) sample using eqn (8).

$$\Delta E^* = \left[ (\Delta L^*)^2 + (\Delta a^*)^2 + (\Delta b^*)^2 \right]^{1/2} \tag{8}$$

### Microstructure

A Nikon Eclipse 80i light microscope (Nikon, Tokyo, Japan), in bright field mode, was selected to study the microstructure of the samples. 4× objective lenses were used to visualise the samples. The images were acquired at a resolution of 1280 × 1024 pixels using NIS-Elements software (Version 4.0, Nikon). The images were analysed using the software ImageJ (U.S. National Institutes of Health, Bethesda, MD, USA).

### Soluble tannin content (STC)

The STC was determined in the ethanolic extract according to the methodology described by Hosseini-nejad *et al.* (2022b). The results were expressed in dry basis as g of gallic acid equivalent (GAE)/100 g db.

### Total carotenoid content (TCC)

The TCC was determined in the lipidic extract (extracted with acetone and diethyl ether) according to

Nath *et al.* (2018). The results were expressed in dry basis as mg  $\beta$ -carotene/100 g db.

### Antioxidant activity (FRAP and DPPH)

Antioxidant activity was studied using the FRAP method in ethanolic extract and the DPPH method in the ethanolic and lipidic extracts, according to Benzie & Strain (1996) and Matsumura *et al.* (2016), respectively. The results were expressed as  $\mu$ mol Trolox eq/g db and % of DPPH inhibition, respectively.

### Statistical analysis

An analysis of variance (ANOVA) was performed using the least significant difference (LSD) test with a 95% confidence interval to compare test means (Statgraphics Centurion XVII Manugistics, Inc., Rockville, MA, USA).

## Results and discussion

### Water sorption and glass transition

The parameters of the sorption models, BET, GAB, Henderson and Caurie, fitted to the experimental data, are shown in Table 1.

The GAB model, widely used in the prediction of water sorption in food systems, with the highest  $R^2$ , was selected to predict the water sorption behaviour (Fig. 1).

Regarding powder stability, the monolayer moisture content has often been described as a critical parameter. However, controlling the glass transition is crucial to ensure the stability and quality of food powders during storage. The glass transition temperature of the persimmon peel powder decreased with increasing water content and the corresponding  $a_w$ . Specifically,

**Table 1** Parameters of the sorption models (BET, GAB, Henderson and Caurie) fitted to experimental data

Model	Parameters	
BET	$w_o$ (g water g <sup>−1</sup> dry solids)	0.089
	$C$	1.294
	$R^2$	0.996
GAB	$w_o$ (g water g <sup>−1</sup> dry solids)	0.098
	$C$	1.318
	$K$	0.937
	$R^2$	0.999
Henderson	$n$	0.783
	$f$	−1.309
	$R^2$	0.998
Caurie	$w_s$ (g water g <sup>−1</sup> dry solids)	0.052
	$r$	44.818
	$R^2$	0.997

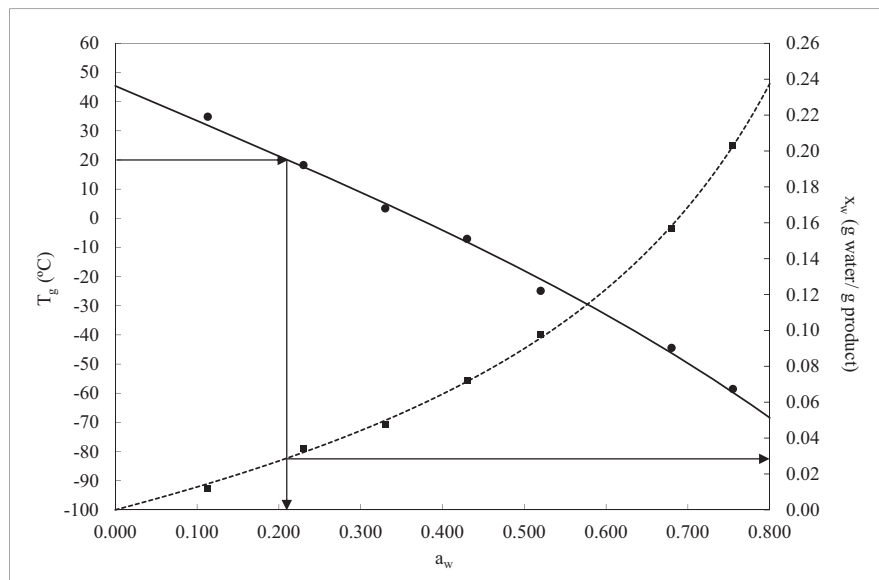


**Figure 1** Glass transition temperature ( $T_g$ ) – water activity ( $a_w$ ) relationship (continuous line) and water activity ( $a_w$ ) – water content relationship ( $x_w$ ) (discontinuous line) of dried persimmon peel powders.

the value of  $T_g$  decreased from 34.8 to  $-58.5$  when  $a_w$  varied from 0.113 to 0.755 (Fig. 1). The low  $T_g$  values obtained are explained by the high concentration of reducing sugars with low molecular weight, 51 g of reducing sugars/100 g of persimmon peel powder according to Hwang *et al.* (2011). Ferrari *et al.* (2021) obtained similar values in mango peel powder ( $T_g = 42.40$  °C at  $a_w = 0.112$  and  $-47.60$  °C at  $a_w = 0.753$ ), with 35 g reducing sugars/100 g.

When the  $T_g$  value is lower than the storage temperature, the glass transitions from glassy to a rubbery state occurs. The relationship between the water content of the persimmon peel powder and its  $T_g$  was fit by the Gordon and Taylor equation (eqn (5)), obtaining the parameters  $T_{g(as)} = 45.402$  °C and  $k = 5.487$  ( $R^2 = 0.996$ ). These values were similar to the obtained in lyophilised persimmon slices (González *et al.*, 2020), hot-air-dried mango peel powders (Ferrari *et al.*, 2021), and lyophilised grapefruit powder (Moraga *et al.*, 2012).

To determine the critical values of water content (CWC) and water activity (CWA) related to glass transition, the combined  $T_g$ - $x_w$ - $a_w$  data and the Gordon and Taylor and GAB fitted models were used (Fig. 1). At 20 °C, the CWA value was 0.211 and the corresponding CWC was 0.029 g water g<sup>-1</sup> product. Therefore, to keep the persimmon peel powder in a glassy state, the relative humidity (RH) of the environment in contact with the sample should be lower than 21.1%, and the water content lower than 0.029 g water g<sup>-1</sup> product. Similar values were obtained by González

*et al.* (2020) in freeze-dried persimmon slices (CWA = 0.165 and CWC = 0.031 g water g<sup>-1</sup> product). Furthermore, in a study performed in freeze-dried grapefruit powder, these values were 0.140 and 0.043 g water g<sup>-1</sup> product, respectively (Moraga *et al.*, 2012). In all cases, CWC values were lower than  $w_o$ , so the monolayer moisture content cannot assure the powder preservation during storage.

At refrigeration storage conditions (i.e. 5 °C), the expected CWA and CWC values would be higher (0.331 and 0.050 g water g<sup>-1</sup> product, respectively), thus increasing the stability range (Fig. 1).

### Mechanical properties

The penetration test performed on the samples allowed to detect changes in the mechanical properties related to the different  $a_w$  levels (Table 2).

Low  $a_w$  preserved the product with characteristics of a free-flowing powder, and as the wetting process progressed, collapse-related phenomena, such as stickiness and caking, were observed. Hardening occurred first, going from a free-flowing powder below CWC or CWA to a product with significantly higher force and area values.

The change from a glassy to a rubbery state at  $a_w$  of 0.211 led to a significant increase ( $P < 0.05$ ) in both mechanical parameters, reaching the highest values at  $a_w$  of 0.430. The sample with  $a_w$  of 0.230 (in the rubbery state) presented a value of area significantly higher than the sample with  $a_w$  of 0.113 (in the glassy



**Table 2** Maximum force (N), compression area (N·mm) and colour parameters ( $L^*$ ,  $h^*$ ,  $C^*$ ,  $\Delta E^*$ ) of persimmon peel powder at different water activities

Samples	Force (N)	Area (N·mm)	$L^*$	$h^*$	$C^*$	$\Delta E^*$
$a_w = 0.113$	$0.51^c \pm 0.14$	$0.55^d \pm 0.12$	$77.98^a \pm 0.49$	$79.52^a \pm 0.73$	$28.37^b \pm 0.24$	–
$a_w = 0.230$	$0.48^c \pm 0.01$	$0.92^c \pm 0.31$	$70.93^b \pm 0.73$	$74.45^b \pm 0.35$	$38.84^a \pm 1.27$	12.96
$a_w = 0.330$	$1.71^b \pm 0.14$	$2.08^b \pm 0.18$	$64.01^c \pm 0.71$	$72.27^c \pm 0.35$	$38.30^a \pm 0.45$	17.15
$a_w = 0.430$	$2.44^a \pm 0.25$	$2.43^a \pm 0.29$	$61.25^d \pm 0.35$	$69.30^d \pm 0.15$	$38.15^a \pm 0.26$	20.24
$a_w = 0.520$	$0.49^c \pm 0.10$	$0.40^d \pm 0.09$	$61.64^d \pm 0.14$	$71.40^c \pm 0.19$	$38.04^a \pm 0.28$	19.55
$a_w = 0.680$	$0.38^c \pm 0.01$	$0.29^d \pm 0.09$	$52.46^e \pm 0.65$	$59.89^f \pm 0.87$	$24.78^d \pm 0.42$	27.30
$a_w = 0.755$	$0.45^c \pm 0.05$	$0.35^d \pm 0.04$	$51.62^e \pm 0.27$	$63.37^e \pm 0.82$	$25.56^c \pm 0.57$	27.56

Values in a column with different superscripts differ significantly ( $P < 0.05$ ) according to ANOVA.

state), even though no significant changes were observed in the maximum force values. This is associated with the beginning of the structure collapse process, which is related to the formation of bridges between particles, causing them to stick together (Aguilera *et al.*, 1995). As the wetting process continues, crystallisation may occur, and moisture released from the crystallised to the amorphous regions accelerates the caking process. The rate of caking is a function of the difference between the storage temperature and the  $T_g$ , being faster as  $T - T_g$  ( $\Delta T$ ) increases (Roos *et al.*, 1998). From a  $a_w$  of 0.520, a significant decrease ( $P < 0.05$ ) in both mechanical parameters was observed, which reflects the softening of the matrix, as an extension of the structure collapse. Therefore, the glass transition exhibits a significant change in the mechanical properties of the persimmon peel powder and must be considered as a critical parameter to avoid caking.

**Colour**

Regarding the colour evolution of the persimmon peel powder samples at the different  $a_w$  levels, Table 2 shows the colour attributes luminosity ( $L^*$ ), hue angle ( $h^*$ ), chroma ( $C^*$ ) and total colour differences ( $\Delta E^*$ ).

The  $L^*$  values decreased significantly ( $P < 0.05$ ) with the increase in  $a_w$ , which indicates that samples became darker when the water content and the  $a_w$

were higher. The values of  $h^*$  decreased with increasing the  $a_w$ , indicating that the samples turned reddish as water content increased. Regarding the  $C^*$  values, an increase from  $a_w = 0.113$  to  $a_w = 0.230$  was observed, which could be attributed to the different physical state. No significant differences ( $P > 0.05$ ) were observed in the  $C^*$  values from  $a_w = 0.230$  to  $a_w = 0.520$ ; and beyond that  $a_w$  value a significant decrease ( $P < 0.05$ ) was found.

Total colour differences were evaluated regarding the sample with the lowest  $a_w$  (Table 2). As all  $\Delta E^*$  values were higher than 12.96, all differences can be considered perceptible to the human eye (Obón *et al.*, 2009), as also seen in Fig. 2a. The total colour differences appeared to be related not only to the glass transition but also to the amount of water available, related to the  $a_w$ . Previous findings in similar products showed comparable results, which stated that colour change increases with increasing  $a_w$ , whereas it is minimal in the glassy state due to the slow diffusion of reactants (Telis & Martínez-Navarrete, 2010; Moraga *et al.*, 2011; Al-Ghamdi *et al.*, 2020; González *et al.*, 2020).

During fruit storage, both enzymatic and non-enzymatic browning may occur. Enzymatic browning, caused by the action of polyphenol oxidase, can be inhibited at low  $a_w$ . Thus, colour changes in low  $a_w$  samples can be attributed mostly to the non-enzymatic browning reaction, which occurs due to the concentration and interactions of sugars and amino acids in the

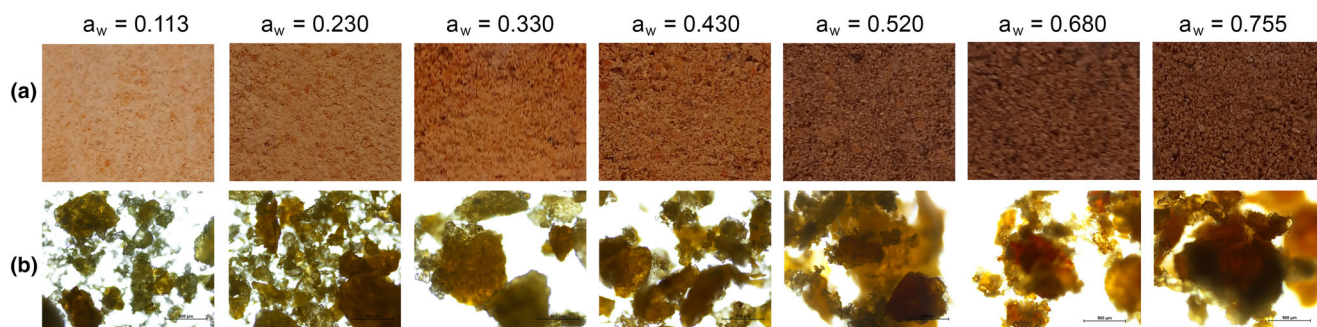


**Figure 2** Photographs (a) and light microscopy images (b) of the persimmon peel powder at the different  $a_w$  values.

fruit. The sharp increase in the  $\Delta E^*$  values of the samples with  $a_w = 0.680$  is related to the maximum reaction rate for non-enzymatic browning, which occurs at  $a_w$  0.65–0.70, and has been attributed to a balance of viscosity-controlled diffusion, dilution and concentration effects. Furthermore, the rate of enzymatic browning reactions is also amplified under these conditions (Labuza *et al.*, 1972).

### Light microscopy

Light microscopy images of the persimmon peel powder at the different  $a_w$  values are presented in Fig. 2b. The persimmon peel powders were observed as individual particles when the  $a_w$  values were low ( $a_w = 0.113$  and  $a_w = 0.230$ ) with a mean particle area of  $185 \mu\text{m}^2$ . However, when  $a_w$  increased from 0.330 to 0.755, a more agglomerated peel powder was observed, losing their individuality and increasing the mean particle area (over  $400 \mu\text{m}^2$ ). These images corroborate the findings observed in the mechanical changes related to the glass transition. In the rubbery state, the formation of an incipient liquid state of lower viscosity on the particle surface leads to stickiness, interparticle bridging, agglomeration and structure collapse.

### Soluble tannin content (STC) and antioxidant activity

Table 3 shows the STC, and the antioxidant activity determined using FRAP and DPPH methods in the ethanolic extract of the persimmon peel powder samples as a function of the  $a_w$ . The sample with  $a_w = 0.430$  showed the highest STC value ( $P < 0.05$ ), followed by the samples with lower  $a_w$  (0.113 and 0.230).

Increasing  $a_w$  above 0.430 led to a decrease in STC values, which could be attributed to an increase in the rate of enzymatic browning reactions favoured at high  $a_w$ , which favours enzyme-substrate interactions. Furthermore, this decrease in STC could also be related to the polymerisation of the phenols, which would

become insoluble due to higher water mobility. The observed evolution of the STC content appears to be related to glass transition and the availability of water, which helps molecular mobility and thus supports degradation and polymerisation reactions.

Regarding the antioxidant capacity, measured by the FRAP method, the results are strongly correlated with the STC content. The highest antioxidant capacity was presented by samples with an  $a_w$  of 0.330 and 0.430, without significant differences ( $P > 0.05$ ) between them, followed by the samples with low  $a_w$  (0.113 and 0.230). As the  $a_w$  increased above 0.430, the antioxidant capacity decreased; the higher the  $a_w$ , the lower the value of FRAP. The pattern is consistent with studies conducted on freeze-drying persimmon slices during its storage at different RH (González *et al.*, 2020).

Regarding the antioxidant capacity, measured by the DPPH method, no significant differences were found among samples with  $a_w$  from 0.113 to 0.430 ( $P > 0.05$ ). A sharp decrease in the percentage of inhibition ( $P < 0.05$ ) was observed at higher  $a_w$  values. A similar trend was observed in freeze-dried grapefruit powder, where a negative linear correlation was found between antioxidant capacity, measured by the DPPH method, and RH (Moraga *et al.*, 2012).

### Total carotenoid content (TCC) and antioxidant activity

Table 3 shows the content of TCC, and the antioxidant activity measured in the lipid extract using DPPH method. As is well known, carotenoids are sensitive to various factors, including oxygen, light, temperature and water content. In our study, the content of TCC, expressed as a dry basis, was significantly different ( $P < 0.05$ ) between samples. The sample with  $a_w = 0.520$  showed the highest TCC values ( $P < 0.05$ ), followed by the samples with  $a_w = 0.430$  and  $a_w = 0.330$ . Lavelli *et al.* (2007) obtained similar results in freeze-dried carrots, where the rate of carotenoid degradation was at a minimum over the  $a_w$  range 0.31–0.54

Samples	Ethanolic extract			Lipidic extract	
	STC (g GAE/100 g db)	FRAP ( $\mu\text{mol}$ Trolox per g db)	DPPH (% inhibition)	TCC (g $\beta$ -carotene/100 g db)	DPPH (% inhibition)
$a_w = 0.113$	$0.58^b \pm 0.13$	$81.86^b \pm 0.96$	$92.43^a \pm 0.13$	$0.076^f \pm 0.010$	–
$a_w = 0.230$	$0.55^b \pm 0.03$	$78.64^b \pm 3.76$	$93.94^a \pm 0.57$	$0.156^d \pm 0.022$	$8.14^b \pm 1.33$
$a_w = 0.330$	$0.46^c \pm 0.06$	$107.92^a \pm 1.34$	$95.16^a \pm 0.38$	$0.257^c \pm 0.015$	$4.48^c \pm 1.57$
$a_w = 0.430$	$0.75^a \pm 0.12$	$109.62^a \pm 1.44$	$94.35^a \pm 0.72$	$0.300^b \pm 0.016$	$5.23^c \pm 0.51$
$a_w = 0.520$	$0.33^d \pm 0.05$	$49.16^c \pm 1.48$	$74.91^b \pm 3.81$	$0.347^a \pm 0.012$	$11.29^a \pm 3.63$
$a_w = 0.680$	$0.30^d \pm 0.09$	$23.80^d \pm 1.13$	$31.15^c \pm 3.33$	$0.110^e \pm 0.008$	$5.29^c \pm 4.28$
$a_w = 0.755$	$0.11^e \pm 0.04$	$10.50^e \pm 1.33$	$13.86^d \pm 1.07$	$0.159^d \pm 0.006$	$5.11^c \pm 1.42$

Values in a column with different superscripts differ significantly ( $P < 0.05$ ) according to ANOVA.

**Table 3** Soluble tannin content (STC), total carotenoid content (TCC) and antioxidant activity (FRAP and DPPH) in the ethanolic and lipidic extracts of persimmon peel powder at different water activities

in blanched and unblanched samples. The persimmon peel powder with  $a_w = 0.113$  showed the lowest ( $P < 0.05$ ) TCC value, followed by the sample with  $a_w = 0.680$ ; no significant differences ( $P > 0.05$ ) were found between samples with  $a_w = 0.730$  and  $0.230$ . Regarding antioxidant capacity, measured by the DPPH method, the results are highly correlated with TCC content; the highest ( $P < 0.05$ ) antioxidant capacity was found in samples with  $a_w = 0.520$ .

Carotenoids degradation followed the U-shaped pattern typical of lipid oxidation, with a high deterioration rate at extreme low and high moisture contents. The decrease in the oxidation rate to a minimum, as  $a_w$  increases from the dry state, has been related to the capacity of water to replace oxygen within the sorption surface, to quench free radicals or to form hydration spheres around metal ions (Labuza & Dugan, 1971; Quast *et al.*, 1972). Therefore, low water activities, although can stabilise reactions, do not prevent carotenoids from degradation. In this sense, it would be recommended to use multi-layer laminates for packaging the product, incorporating materials such as aluminium and other barrier films that offer protection against moisture, oxygen and light.

### Conclusions

The physical properties and concentration of bioactive compounds of the persimmon peel powder obtained through hot-air drying are greatly influenced by the  $a_w$  and the glass transition temperature. This study led to some practical points about the processing and storage conditions required to maintain this ingredient with a high quality. Storing the powder in a glassy state (at 20 °C below  $a_w = 0.211$  and  $0.029$  g water g<sup>-1</sup> product) allows to obtain a free-flowing powder with a high content of phenolic compounds and antioxidant capacity. Above a  $a_w = 0.520$ , the increase in degradation reactions leads to a significant decrease in the content of bioactive compounds. This work paves the way for using persimmon by-products to produce a potential functional and sustainable ingredient that can be used in the food industry.

### Acknowledgments

This research was funded by MCIN/AEI/10.13039/501100011033, and by ‘ERDF A way of making Europe’ grant number RTA2017-00045-C02-02. The authors thank Phillip Bentley for his assistance in correcting the English of the manuscript.

### Author contributions

**Sepideh Hosseininejad:** Writing – original draft; investigation; data curation. **Virginia Larrea Santos:** Investigation; methodology. **Amparo Quiles:** Investigation;

methodology. **Isabel Hernando:** Conceptualization; writing – review and editing; formal analysis; supervision. **Gemma Moraga:** Conceptualization; writing – review and editing; project administration; supervision; resources; formal analysis.

### Conflicts of interest

The authors declare that they have no conflict of interest.

### Ethical guidelines

Ethics approval was not required for this research.

### Peer review

The peer review history for this article is available at <https://www.webofscience.com/api/gateway/wos/peer-review/10.1111/ijfs.16982>.

### Data availability statement

The data used to support the findings of this study can be made available by the corresponding author upon request.

### References

Aguilera, J.M., Valle, J.M. & Karel, M. (1995). Caking phenomena in amorphous food powders. *Food Science and Technology*, **6**, 149–155.

The authors reviewed the literature to report the main factors influencing the caking of free-flowing powders during storage. They highlighted the relationships between storage-induced caking and the glass transition of amorphous powders, which was important to comprehend our results on mechanical properties.

Al-Ghamdi, S., Hong, Y.K., Qu, Z. & Sablani, S.S. (2020). State diagram, water sorption isotherms and color stability of pumpkin (*Cucurbita pepo* L.). *Journal of Food Engineering*, **273**, 1–8.

Bahloul, N., Boudhrioua, N. & Kechaou, N. (2008). Moisture desorption-adsorption isotherms and isosteric heats of sorption of Tunisian olive leaves (*Olea europaea* L.). *Industrial Crops and Products*, **28**, 162–176.

Benzie, I.F.F. & Strain, J.J. (1996). The ferric reducing ability of plasma (FRAP) as a measure of antioxidant power: the FRAP assay. *Analytical Biochemistry*, **239**, 70–76.

Collazos-Escobar, G.A., Gutiérrez-Guzmán, N., Váquiro-Herrera, H.A., Bon, J. & Garcia-Perez, J.V. (2022). Thermodynamic analysis and modeling of water vapor adsorption isotherms of roasted specialty coffee (*Coffea arabica* L. cv. Colombia). *LWT - Food Science and Technology*, **160**, 113335.

Del Rio Osorio, L., Flórez-López, E. & Grande-Tovar, C. (2021). The potential of selected agri-food loss and waste to contribute to a circular economy: applications in the food, cosmetic and pharmaceutical industries. *Molecules*, **26**, 515.

FAO. (2021). *Food wastage footprint. Impacts on natural resources*. FAO. <http://www.fao.org/faostat/en/#data/QC/visualize>

Ferrari, C.C., Morgano, M.A. & Germer, S.P.M. (2021). Evaluation of water sorption isotherm, glass transition temperature, vitamin C and color stability of mango peel powder during storage. *SN Applied Sciences*, **3**, 1–12.

The authors reported the physical and chemical stability of the mango peel powder produced by hot-air drying. Sorption isotherms at 25 °C and glass transition temperatures ( $T_g$ ) of the samples in equilibrium at different  $a_w$  were determined. Their results helped us understand the results of our work, mainly those related to water sorption and glass transition.

González, C.M., Llorca, E., Quiles, A., Hernando, I. & Moraga, G. (2020). Water sorption and glass transition in freeze-dried persimmon slices. Effect on physical properties and bioactive compounds. *LWT - Food Science and Technology*, **130**, 1–8.

Gorinstein, S., Zachwieja, Z., Foltá, M. *et al.* (2001). Comparative contents of dietary fiber, total phenolics, and minerals in persimmons and apples. *Journal of Agricultural and Food Chemistry*, **49**, 952–957.

Hosseininejad, S., González, C.M., Hernando, I. & Moraga, G. (2022a). Valorization of persimmon fruit through the development of new food products. *Frontiers*, **2**, 1–10.

Hosseininejad, S., Larrea, V., Moraga, G. & Hernando, I. (2022b). Evaluation of the bioactive compounds, and physicochemical and sensory properties of gluten-free muffins enriched with persimmon 'Rojo Brillante' flour. *Food*, **11**, 1–13.

Hwang, I., Jeong, M. & Chung, S. (2011). The physicochemical properties and the antioxidant activities of persimmon peel powders with different particle sizes. *Applied Biological Chemistry*, **54**, 442–446.

Krokida, M.K. & Marinos-Kouris, D. (2003). Rehydration kinetics of dehydrated products. *Journal of Food Engineering*, **57**, 1–7.

Labuza, T. & Dugan, L.R. (1971). Kinetics of lipid oxidation in foods. *Food Science & Nutrition*, **2**, 385–405.

Labuza, T., McNally, L., Gallagher, D., Hawkes, J. & Hurado, F. (1972). Stability of intermediate moisture oxidation introduction. *Stability of Intermediate Moisture Foods*, **37**, 154–159.

Lavelli, V., Zannoni, B. & Zaniboni, A. (2007). Effect of water activity on carotenoid degradation in dehydrated carrots. *Food Chemistry*, **104**, 1705–1711.

The authors studied the effect of water activity on the stability of carotenoids in dehydrated carrots. This work helped to understand the results related to carotenoid oxidation.

Matsumoto, T., Matsuzaki, H., Takata, K., Tsurunaga, Y., Takahashi, H. & Kurahashi, T. (2007). Inhibition of astringency removal in semidried Japanese persimmon fruit by 1-methylcyclopropene treatment. *HortScience*, **42**, 1493–1495.

Matsumura, Y., Ito, T., Yano, H. *et al.* (2016). Antioxidant potential in non-extractable fractions of dried persimmon (*Diospyros kaki* Thunb.). *Food Chemistry*, **202**, 99–103.

Miller, K.L., Liebowitz, R.S., Newby, L.K. & Durham, M.H.S. (2004). Complementary and alternative medicine in cardiovascular disease: a review of biologically based approaches. *American Heart Journal*, **147**, 401–411.

Moraga, G., Talens, P., Moraga, M. & Martínez-Navarrete, N. (2011). Implication of water activity and glass transition on the mechanical and optical properties of freeze-dried apple and banana slices. *Journal of Food Engineering*, **106**, 212–219.

Moraga, G., Igual, M., García-Martínez, E., Mosquera, L.H. & Martínez-Navarrete, N. (2012). Effect of relative humidity and storage time on the bioactive compounds and functional properties of grapefruit powder. *Journal of Food Engineering*, **112**, 191–199.

The modified state diagram for freeze-dried grapefruit powder was obtained to identify the critical water content and critical water activity triggering the amorphous matrix's glass transition. The authors reported that ensuring the glassy state helped mitigate deteriorative reactions associated with the loss of bioactive compounds in the powders, which is in line with our results.

Nath, P., Kale, S.J., Kaur, C. & Chauhan, O.P. (2018). Phytonutrient composition, antioxidant activity and acceptability of muffins incorporated with red capsicum pomace powder. *Journal of Food Science and Technology*, **55**, 2208–2219.

Obón, J.M., Castellar, M., Alacid, M. & Fernández-López, J. (2009). Production of a red – purple food colorant from *Opuntia stricta* fruits by spray drying and its application in food model systems. *Journal of Food Engineering*, **90**, 471–479.

Oh, H.J., Park, M.S., Cho, K.J., Choi, S.I. & Kang, H.M. (2018). Geographical indication and development plans in South Korea: a study on dried persimmons. *Forest Science and Technology*, **14**, 41–46.

Ohguchi, K., Nakajima, C., Oyama, M. *et al.* (2010). Inhibitory effects of flavonoid glycosides isolated from the peel of Japanese persimmon (*Diospyros kaki* Fuyu) on antigen-stimulated degranulation in rat basophilic leukaemia RBL-2H3 cells. *Biological and Pharmaceutical Bulletin*, **33**, 122–124.

Perez-Pirotto, C., Moraga, G., Hernando, I., Cozzano, S. & Arica, P. (2022). Sorption isotherms, glass transition and bioactive compounds of ingredients enriched with soluble fibre from orange pomace. *Food*, **11**, 1–14.

Quast, D.G., Karel, M. & Rand, W.M. (1972). Development of a mathematical model for oxidation of potato chips as a function of oxygen pressure, extent of oxidation and equilibrium relative humidity. *Nutrition & Food Science*, **37**, 673–678.

Raskin, I., Ribnicky, D.M., Komarnytsky, S. *et al.* (2002). Plants and human health in the twenty-first century. *Biotechnology*, **20**, 522–531.

Roos, Y.H. (1995). Characterization of food polymers using state diagrams. *Journal of Food Engineering*, **24**, 339–360.

Roos, Y.H., Roininen, K., Jouppila, K. & Tuorila, H. (1998). Glass transition and water plasticization effects on crispness of a snack food extrudate. *International Journal of Food Properties*, **1**, 163–180.

Smrke, T., Persic, M., Veberic, R., Sircelj, H. & Jakopic, J. (2019). Influence of reflective foil on persimmon (*Diospyros kaki* Thunb.) fruit peel colour and selected bioactive compounds. *Scientific Reports*, **8**, 1–8.

Suzuki, T., Someya, S., Hu, F. & Tanokura, M. (2005). Comparative study of catechin compositions in five Japanese persimmons (*Diospyros kaki*). *Food Chemistry*, **93**, 149–152.

Telis, V.R.N. & Martínez-Navarrete, N. (2010). Application of compression test in analysis of mechanical and color changes in grapefruit juice powder as related to glass transition and water activity. *LWT - Food Science and Technology*, **43**, 744–751.

Yaqub, S., Farooq, U., Shafi, A. *et al.* (2016). Chemistry and functionality of bioactive compounds present in persimmon. *Journal of Chemistry*, **2016**, 1–13.

Ye, H., Luo, L., Wang, J., Jiang, K., Yue, T. & Yang, H. (2022). Highly galloylated and A-type prodelphinidins and procyanidins in persimmon (*Diospyros kaki* L.) peel. *Food Chemistry*, **378**, 131972.